



## INVESTIGATION OF CONVECTION HEAT TRANSFER FOR HIGH INTEGRAL FINNED TUBE HEAT EXCHANGER

Dr. Muna Sabah Kassim<sup>1</sup>, \*Hadeer Sattar Gaber<sup>2</sup>

1. Assistant Prof., Mechanical Engineering Department, Mustansiriyah University, Baghdad, Iraq.
2. M.Sc.Student Mechanical Engineering, Department, Mustansiriyah University, Baghdad, Iraq.

Received 28/5/2018

Accepted in revised form 9/10/2018

Published 1/11/2019

**Abstract:** Numerical investigation has been performed in this work to evaluate the performance for triangular finned tube heat exchanger. In numerical work, the effect of space (2.5, 3 and 3.5 mm) distance between every two finned shaped and the volumetric flow rate on the heat transfer coefficient are examined consists of cold water loop, hot air loop and the test section which is a concentric parallel flow double pipe heat exchanger. Coldwater and hot air are used as working fluids in the tube side and shell side, respectively. water at Reynold's numbers ranging from (3019.892 to 8035.044 ) flows through the inner tube. The inlet cold water temperatures are (45, 35, 25 and 15) °C respectively. Numerical simulation has been carried out on present heat exchanger to analyze both flow field and heat transfer using ANSYS, FLUENT15 computational fluid dynamic (CFD) package model. The finned tubes provide higher Nusselt numbers than the smooth tube. In the less pitch ( $p=2.5\text{mm}$ ) compared with other pitch.

**Keywords:** *Nusselt, Finned tube, Reynold's number, ANSYS.*

### تحقيق انتقال الحرارة بالحمل لمبادل حراري ذو أنابيب مزعنة طويلة

**الخلاصة:** تم إجراء بحث عددي في هذا العمل لتقييم أداء المبادل الحراري للأنبوب ذو الزعنة المثلثية. الجانب النظري تضمن فحص تأثير المسافات (2.5، 3 و 3.5) ملم بين زعنفتين متتاليتين ومتتاليتين ومعدل التدفق الحجمي على معامل انتقال الحرارة واختيار أفضل حالة في تحسين انتقال الحرارة، الجانب العملي تضمن بناء جهاز مختبري يتكون من دائرة الهواء الساخن ودائرة الماء البارد والمبادل الحراري ذو الجريان المتوازي وتستخدم المياه الباردة والهواء الساخن كسوائل عمل في جانب الأنابيب وجانب القشرة، على التوالي. يتدفق الماء في أرقام رينولد من (3019.892 إلى 8035.044) خلال الأنبوب الداخلي درجات حرارة دخول الماء إلى أنبوب الاختبار (45, 35, 25, 15) درجة مئوية محاكاة عددية تم إنجازها للمبادل الحراري لتحليل جريان المائع وانتقال الحرارة باستخدام البرامج المتخصصة (ANSYS, FLUENT15) تم استخدام حل معادلات الاستمرارية والزخم والطاقة لتحليل الجريان خلال المبادل الحراري. مقارنة انتقال الحرارة للأنبوب الملس والمزعنة تم إجرائها حالة الاستقرار، السلوك النيوتني، اللانضغاطية والأبعاد الثلاثية تم افتراضه. النتائج بينت بان إضافة الزعانف يحسن انتقال الحرارة خلال المبادل الحراري.

\*Corresponding Author [hadeersattar@yahoo.com](mailto:hadeersattar@yahoo.com)

## 1. Introduction

Heat exchangers are used in various processes ranging from utilization, conversion and recovery of thermal energy in various industrial, household and commercial uses. Some examples implicate condensation in power, cogeneration plants, cooling in thermal processing of chemical, agricultural products, sensible heating, steam generation, pharmaceutical, squandering heat recovery and liquid warming in industry ionization. improve in heat exchanger's performance can make more frugal design of heat exchanger which can assist to Use of heat transfer enhancement techniques leads to increase in heat transfer coefficient but at the cost of increase in pressure drop. So, while designing a heat exchanger using any of these techniques, analysis of pressure drop and heat transfer rate has to be done.

Apart from these issues like long term performance and detailed economic analysis of heat exchanger, it should to be studied. To probe high heat transfer rate in an existing or new heat exchanger while taking care of the increased several techniques, pumping power have been suggested in modern years and are talk over [1,2] Tube-fins heat exchangers have been used to exchange heat between liquids and gases, which are one or two phases.

The improvement of the tube fins heat exchangers are delimited by the air side heat transfer resistance. This is because the air side heat transfer coefficient is highly little than the liquid side heat transfer coefficient [6]. Hence, to have balanced thermal conductance's on both sides for a reduction size heat exchanger, fins are used on the gas side to increment surface area.

In a tube–fin exchanger, rectangular and round tubes are most public, even though elliptical tubes are as well hired. Fins are mostly hired on the outside but they may be used on the inner of the tubes in some applications [3].

## 2. Literature Survey

Ayad 2011[4] Investigated the heat transfer characteristics of cross flow air cooled single tube multi passes (smooth and integral low finned tube) and its effect on heat transfer enhancement. Two test sections from Perspex duct were designated. Each test section has a test tube (single aluminum tube multi passes) with eight or four passes. The experimental results showed that the air side heat transfer coefficient of the integral low finned tube was higher than that of the smooth tube. The enhancement ratio when using the integral low finned tube was (1.86 to 2.38) for eight and four passes.

Ali et. al. (2014) [5] examined the enhancement of heat transfer over external surface of copper pipe with circular fins attached on the outer surface heat exchanger in rectangular channel with air cross-flow. the experiments included using four types of circular fins with (32 mm) inner diameter, (92 mm) outer diameter and (1 mm) thick attached on copper pipe. Each type has (5) circular fins. The first type has five fins without slanted blades, second type has five slanted blades per one fin, third type has seven slanted blades per one fin and fourth type has nine slanted blades per one fin. From results, Nusselt number for second type is about (11.8 %), third type is about (20.25 %) and with fourth type is about (27.5 %) higher than those for the first type. In

addition, experimental results showed that the fourth type has a good enhancement of heat transfer and fin performance. Moreover, it caused significant reduction in thermal resistance by comparison with first .

Bashar 2016 [6] In this work, the augmentation of convective heat transfer in a single -phase turbulent flow by using triangular fins has been experimentally and numerically investigated. In experimental work, the effect of space (22, 27 and 32 mm) distance between every two fins shaped and the volumetric flow rate on the heat transfer coefficient are examined Many of triangular fins are manufactured from copper. They are installed to the external surface of tube. Having (10mm) length of base, (10mm) height, (1mm) thickness, (22, 27, and 32) mm distance between two fins successive and (15mm) pitch between each two of fins. Thermometers and pressure gauges are connected to the tubes and annular sections. The results obtained from the tubes with triangular fins are compared with the smooth tube heat exchanger. It is found that the triangular fins have a significant effect on the heat transfer augmentations. The result showed that the enhancement of heat dissipation for triangular finned tube is (3.8 to 5.4) times than that of smooth tube at space (22 mm) distance between each two successive fins. While, for space 27 and 32 mm will be (3.5 to 4.9) and (3.2 to 4.5)

Ajay and Subrata 1990 [7] obtained numerically laminar flow and heat transfer magnitudes in a finned tube annulus. External circular fins on the inner tube are periodic. Pressure drop and heat transfer characteristics of the fins are obtained in the periodically fully developed region by varying geometric and flow parameters. Geometric parameters are annulus radius ratio (0.3 to 0.5), fin height / annular gap (0.33 to 0.67) and fin spacing / annular gap (2 to 5). Flow parameters are Reynolds number (100 to 1000) and Prandtl number (1 to 5). Comparisons are made with a plain tube annulus having the same length, heat transfer surface area, volume flow rate, and Reynolds number. The entire inter-fin space was found to be occupied by recirculating flow except at Reynolds numbers less than 500. A major contribution to heat transfer is made from the fin side at the downstream end. At Prandtl numbers less than 2, the use of fins may not be justified because the increase in pressure drop is more pronounced than the increase in heat transfer. At a Reynolds number of 1000 and a Prandtl number of 5, the heat transfer increases by a factor of 3.1, while the pressure drop increases by a factor of 2.3.

Torikoshi et al.1995 [8] investigated numerically the tube diameter effect on heat transfer and flow behaviour for a two-row staggered arrangement of plate finned-tubes. In contrast to the circular finned-tubes, the plate fin surface is decreased when the tube diameter increases. It is apparent that the tube diameter effect may be largely ignored for the cases where the diameter is changed only slightly.

Syed et al. 2007 [9] Performed numerical simulation of finned annulus in the steady and laminar convection in the thermal entry region, fully developed flow at uniform heat flux. Finite difference based marching procedure was used to compute the numerical solution of the energy equation. Their results presented Nusselt's number, as a function of dimensionless axial length and thermal entrance length for various configuration of the finned double-pipe. The numerical results showed the Nusselt's

number has complex depending on the geometric variables like ratio of radii, fin height, and number of fins. The validation of the simulation was performed by comparison with open literature.

Iqbal et al. 2013 [10] Investigated the optimal longitudinal fins on the outer surface of the inner pipe enclosed within a concentric outer pipe in laminar and fully developed flow at uniform heat flux. The fin–shape was triangular as the initial profile. The results showed that the optimum fin– shape is dependent on the number of fins, the ration of radii, the number of control points and characteristic length. The enhancement in Nusselt's number was up to 138%,312% and 263% for trapezoidal, triangular and parabolic shapes for equivalent diameter while 212%,59% and 90% respectively for hydraulic diameter. From the historical introduction we observe the study of cross flow air cooled single tube multi passes (smooth and integral low finned tube) and enhancement of heat transfer over external surface its effect on heat transfer enhancement and the effect of space distance between every two fins shaped and the volumetric flow rate on the heat transfer coefficient In the course of these studies and what we have concluded with regard to many effects on heat transfer, we worked on the effect of the distance between the two fins of the same metal along the tube and different fins as well as study the effect in the case of the difference of fins more than a case of more than a distance between the fins and the calculation of form and location The distance on the heat transfer for the air side and the use of more than the value of the contour temperatures.

### 3. Physical Model of System

The system geometry in the present work consists of an integral-finned tube, where the working fluid flows. Different cases have been student in this work, these cases are listed in table (1) .

Table 1. symbols definition

Case	geometry
G04	Smooth tube
G01-P1	External fins tube with pitch (2.5mm)
G01-P2	External fins tube with pitch (3mm)
G01-P3	External fins tube with pitch (3.5mm)
G02-P1	Internal fins tube with pitch (2.5mm)
G02-P2	Internal fins tube with pitch (3mm)
G02-P3	Internal fins tube with pitch (3.5mm)
G03-P1	Internal and external fins with pitch (2.5mm)
G03-P2	Internal and external fins with pitch (3mm)
G03-P3	Internal and external fins with pitch (3.5mm)

#### 3.1 Physical Model of External Finned Tube

Geometry of computational domain with dimensions is illustrated schematically in Fig.(1), internal tube dimensions denoted for inner diameter as ( $d_i$ ) and for outer

diameter as ( $d_o$ ). The number of external triangular fins welded on outer surface for internal diameter determined by using the expression;

$$\text{No. of Fins} = \frac{\text{Outer perimeterr of Internal Tube}}{\text{Required Pitch}} = \frac{\pi d_o}{P} \quad (1)$$

Where ( $P$ ) is the pitch which represent distance from center to center between the neighboring fins, total number of fins in this case is (40 fins). However, the 3D view of the internal tube was presented which in figure (3) has a length of (1000mm), the internal tube designed to carry water flow from inside and imposed to air flow from its outside. Both internal and external tubes have the same length, the external tube modeled to be insulated from the outer side. Fig(1) shows the overall computational domain.

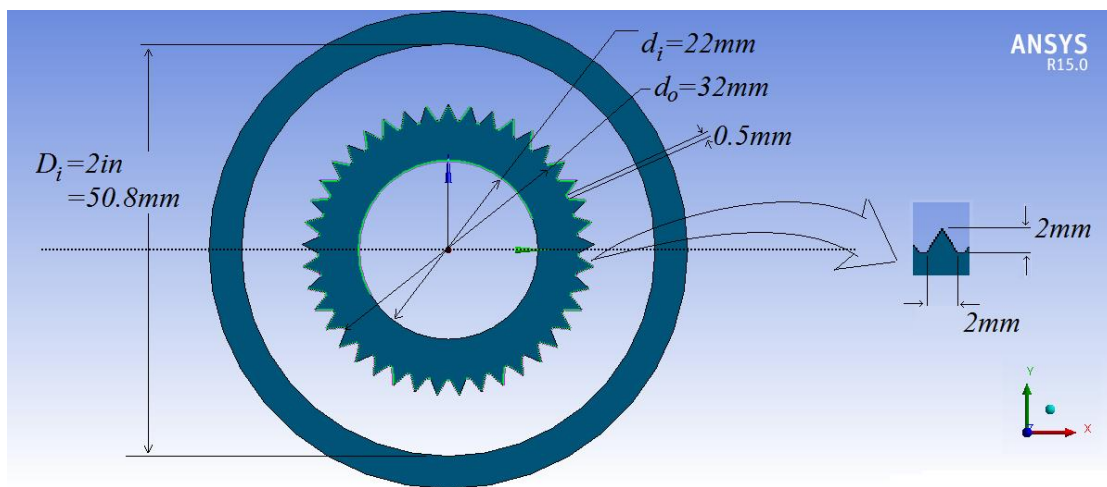


Figure (1). Schematic view of inlet section for domain of G01-P1.

### 3.2 Physical Model of Internal finned Tube

Geometry of computational domain with dimensions is illustrated schematically in Fig.(2). Internal tube, external tube and fins (which is equal to 27 fins) all have the same length of (1m) where the triangular fins welded on the inner surface of internal tube.

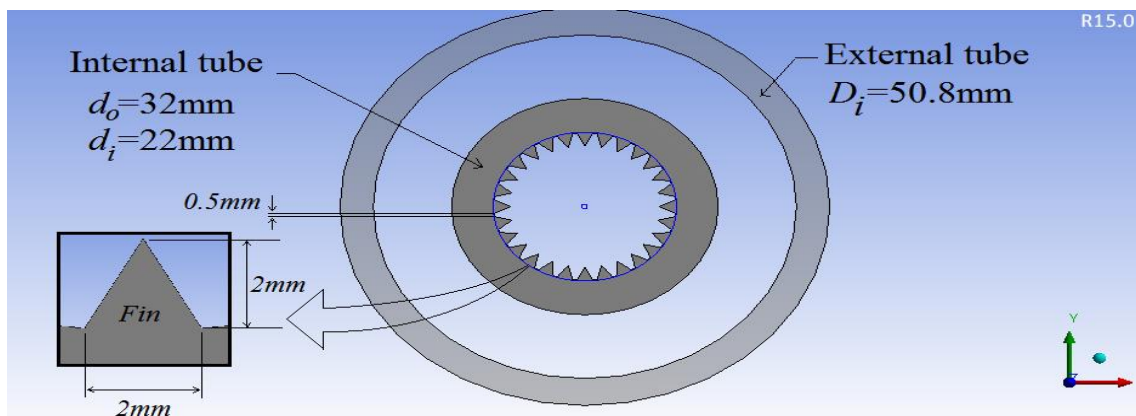


Figure (2). Schematic view of inlet section for domain of G02-P1

### 3.3 Physical Model of Internal and External Finned Tube

The numerical simulated domain is illustrated in Fig. (3) . It's a combination between the two cases (G01-P1 , G02-P1). The external tube has a length of (1000mm) and inner diameter of (50.8mm), it is smooth and insulated from outside. Internal tube also have the same length of external one with inner and outer diameters of (22mm) and (32mm) respectively. The both surfaces are welded to triangular fins with (2mm) high and base width. The distance between each couple of fins is approximately (0.5mm). Therefore, the number of fins on the inner and outer surfaces are (27) and (40) respectively.

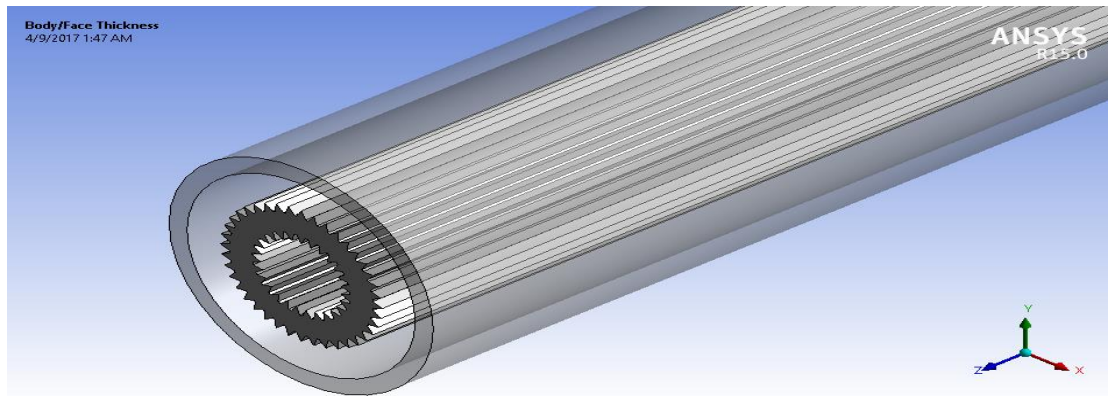


Figure (3). Isometric view of case G03-P1

## 4. Numerical Simulation

Numerical simulation by using ANSYS, FLUENT15 computational fluid dynamic (CFD) package model has been conducted for performing numerical simulation across the heat exchanger using three-dimensional model. The solution of conservation continuity, momentum and energy equations are used to analyze the flow field inside the heat exchanger. A comparison of heat transfer for (smooth, triangular) finned tube, of this work with and without consist integral finned tube heat exchanger with inlet and outlet portions, shown in Figures (4).

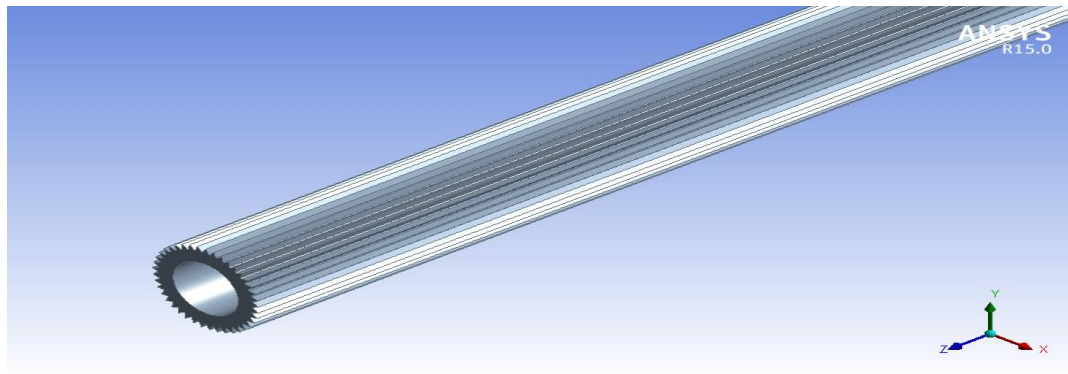


Figure (4). Computational domain G01-P1.

## 5. Governing Equations

The governing differential equation for the fluid flow is given by continuity equation or mass conservation equation, Navier Stokes equation or momentum conservation equation and energy conservation equation. [11]

### 5.1. Continuity Equation

$$\frac{\partial(\rho u)}{\partial x} + \frac{\partial(\rho V)}{\partial y} + \frac{\partial(\rho W)}{\partial z} = 0 \quad (2)$$

### 5.2 Navier Stokes Equation

$$\rho \left( u \frac{\partial u}{\partial x} + V \frac{\partial u}{\partial y} + W \frac{\partial u}{\partial z} \right) = \rho X - \frac{\partial p}{\partial x} + \frac{1}{3} \mu \frac{\partial}{\partial x} \left( \frac{\partial u}{\partial x} + \frac{\partial V}{\partial y} + \frac{\partial W}{\partial z} \right) + \mu \nabla^2 u \quad (3)$$

$$\rho \left( u \frac{\partial V}{\partial x} + V \frac{\partial V}{\partial y} + W \frac{\partial V}{\partial z} \right) = \rho Y - \frac{\partial p}{\partial y} + \frac{1}{3} \mu \frac{\partial}{\partial y} \left( \frac{\partial u}{\partial x} + \frac{\partial V}{\partial y} + \frac{\partial W}{\partial z} \right) + \mu \nabla^2 V \quad (4)$$

$$\rho \left( u \frac{\partial W}{\partial x} + V \frac{\partial W}{\partial y} + W \frac{\partial W}{\partial z} \right) = \rho Z - \frac{\partial p}{\partial z} + \frac{1}{3} \mu \frac{\partial}{\partial z} \left( \frac{\partial u}{\partial x} + \frac{\partial V}{\partial y} + \frac{\partial W}{\partial z} \right) + \mu \nabla^2 W \quad (5)$$

### 5.3 Energy Equation

$$\rho c_p \left( u \frac{\partial T}{\partial x} + V \frac{\partial T}{\partial y} + W \frac{\partial T}{\partial z} \right) = \left( u \frac{\partial P}{\partial x} + V \frac{\partial P}{\partial y} + W \frac{\partial P}{\partial z} \right) + K \nabla^2 T + \mu \phi \quad (6)$$

Where:

$$\phi = 2 \left[ \left( \frac{\partial u}{\partial x} \right)^2 + \left( \frac{\partial V}{\partial y} \right)^2 + \left( \frac{\partial W}{\partial z} \right)^2 \right] + \left[ \left( \frac{\partial u}{\partial y} + \frac{\partial V}{\partial x} \right)^2 + \left( \frac{\partial V}{\partial z} + \frac{\partial W}{\partial y} \right)^2 + \left( \frac{\partial W}{\partial x} + \frac{\partial u}{\partial z} \right)^2 \right] - \frac{2}{3} \left[ \frac{\partial u}{\partial x} + \frac{\partial V}{\partial y} + \frac{\partial W}{\partial z} \right] \quad (7)$$

## 6. Validation

The comparison for Nusselt number between experimental data and Dittus–Boelter correlation. It is noted that the Nusselt number differs by up 5% from the Dittus–Boelter correlation, as show in figure (5).

$$Nu = 0.023(Re)^{4/5}(Pr)^n \quad [12]$$

$n = 0.3$  the process is cooling

where Nu is the Nusselt number, Re is the Reynolds number and Pr is the Prandial number.

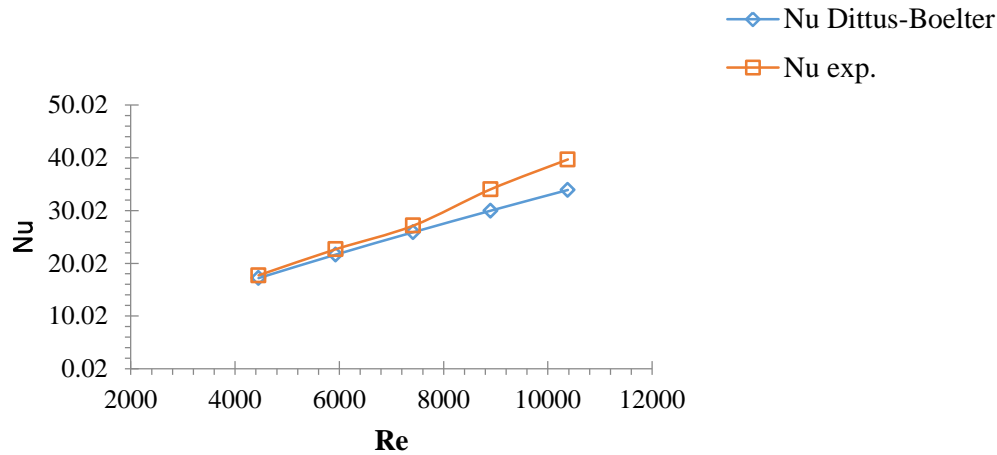


Figure (5). Comparisons experimental data and empirical correlations of the plain tube for Nu.

## 7. Numerical Results Analysis

In this study, the numerical results obtained by ANSYS, FLUENT15 package are presented to show both the flow and heat transfer characteristic in form of temperature and velocity profile for the present models. The results are discussed in the following section.

### 7.1 Velocity Contours

The velocity contours for shell side As seen in the figure (7-b), the flow over longitudinal finned tube with pitch (3.5mm) which is case [G01-P3] increases velocity to 6.314% higher than that in case of smooth tube [G04]( figure (7-a). This increment occurs due to reduction in hydraulic diameter which leads to increase velocity at constant volumetric flow rate. The reduction in hydraulic diameter causes decreasing

in cross sectional area of fluid flow which is resulted in an increase in mean velocity value to satisfy mass conservation equation (which defined as the rate at which mass enters a system is equal to the rate at which mass leaves the system).However, in the case of G01-P2, flow over longitudinal finned tube with pitch (3mm), figure (7-c), the velocity is 7.24% higher than in flow over smooth tube and by 0.93% higher than in flow over finned tube with pith (3.5mm)

Also in the flow over longitudinal finned tube with pitch (2.5mm)[G01-P1], figure (7-d)], the velocity is 9.24%, 2.89% and 1.968% higher than in cases of G04, G01-P3 and G01-P2 respectively.

explained the mean velocity propagation along the shell side at different axial locations. The velocity magnitudes satisfy continuity and momentum conservation as the solution converged in ANSYS solver, the differentiations between cases return to the fact that as pitch decreases between fins lead to increase fins number and as a result, a reduction In air cross sectional area with increasing velocity and decreasing of hydraulic diameter. The different velocity values at inlet and outlet cross sectional areas (locations 0.025m & 0.975m), occur due to the impact of air flow with the tube if the impact region on fin tip or between two fins or over a smooth curvature (as in smooth tube



case), this effect on the stream lines directions and the velocity vectors came from dead zone as appear clearly in figure (7).

Table (2). Velocity magnitudes for different axial locations within shell side with air flow over smooth and finned tubes.

Case	Velocity magnitude (m/s)				
	0.025m (Air Outlet)	0.25m	0.5m	0.75m	0.975m (Air inlet)
Smooth tube (G04)	1.7632	0.7429	0.7438	0.7405	1.1490
Finned tube with pitch (3.5mm) (G01-P3)	1.7880	0.7930	0.7923	0.7897	1.7604
Finned tube with pitch (3mm) (G01-P2)	1.8270	0.8003	0.7997	0.8001	1.7682
Finned tube with pitch (2.5mm) (G01-P1)	1.7837	0.8117	0.8156	0.8130	1.8413

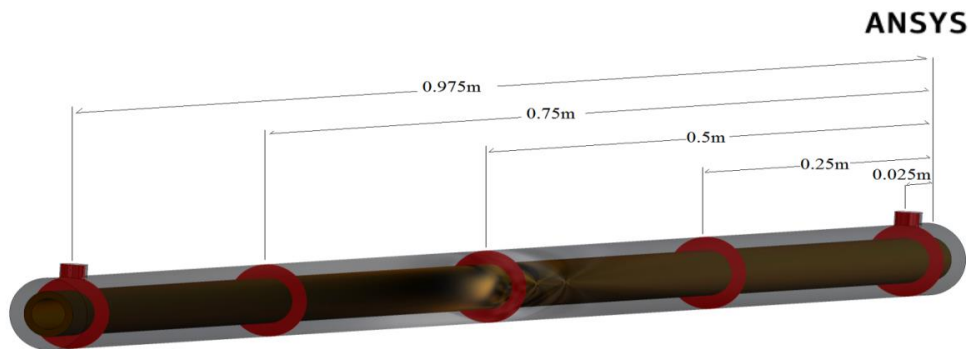


Figure (6); axial locations within shell side

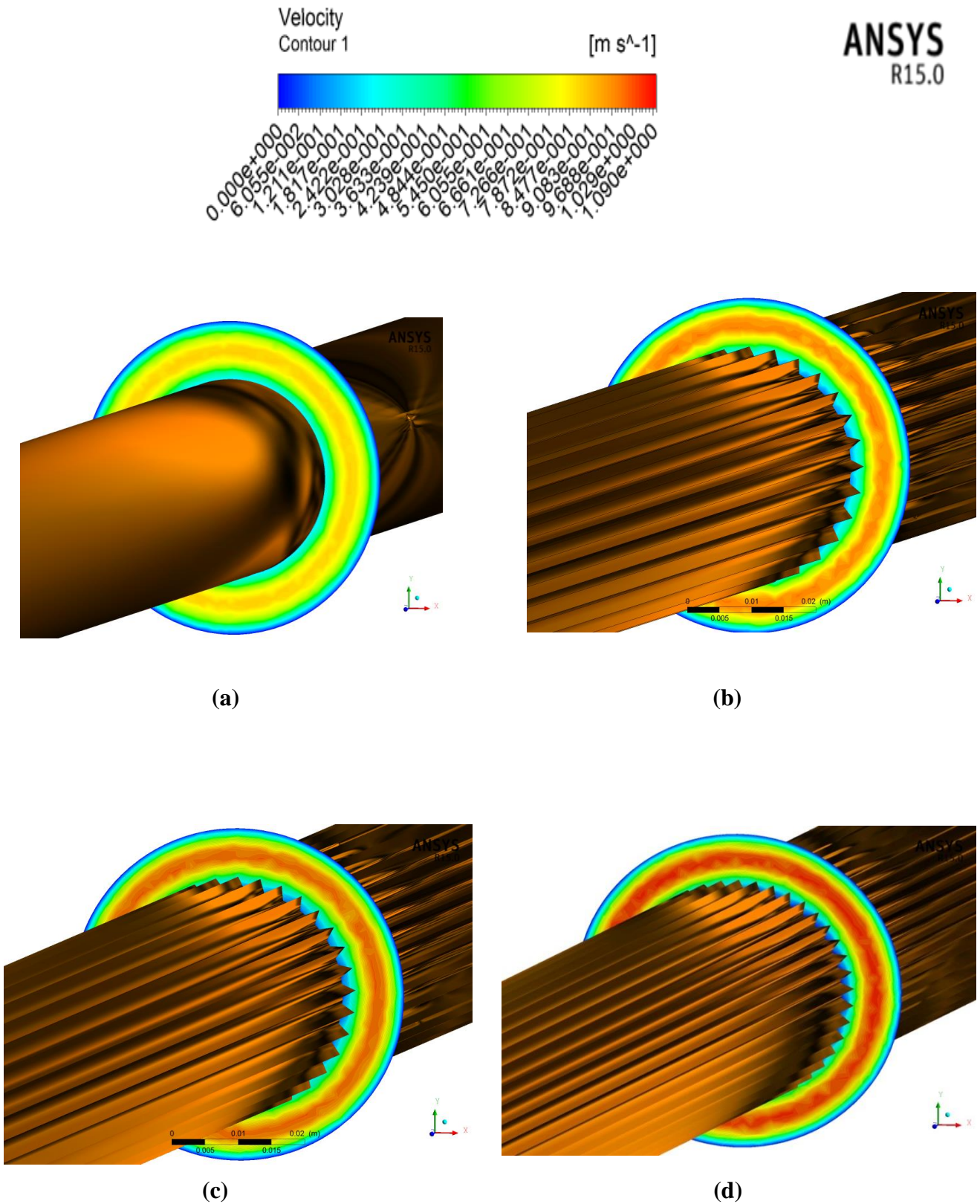


Figure (7); Velocity contours for shell side with air flow over; (a) smooth tube, (b) finned tube with pitch (3.5mm), (c) finned tube with pitch (3mm), (d) finned tube with pitch(2.5mm)

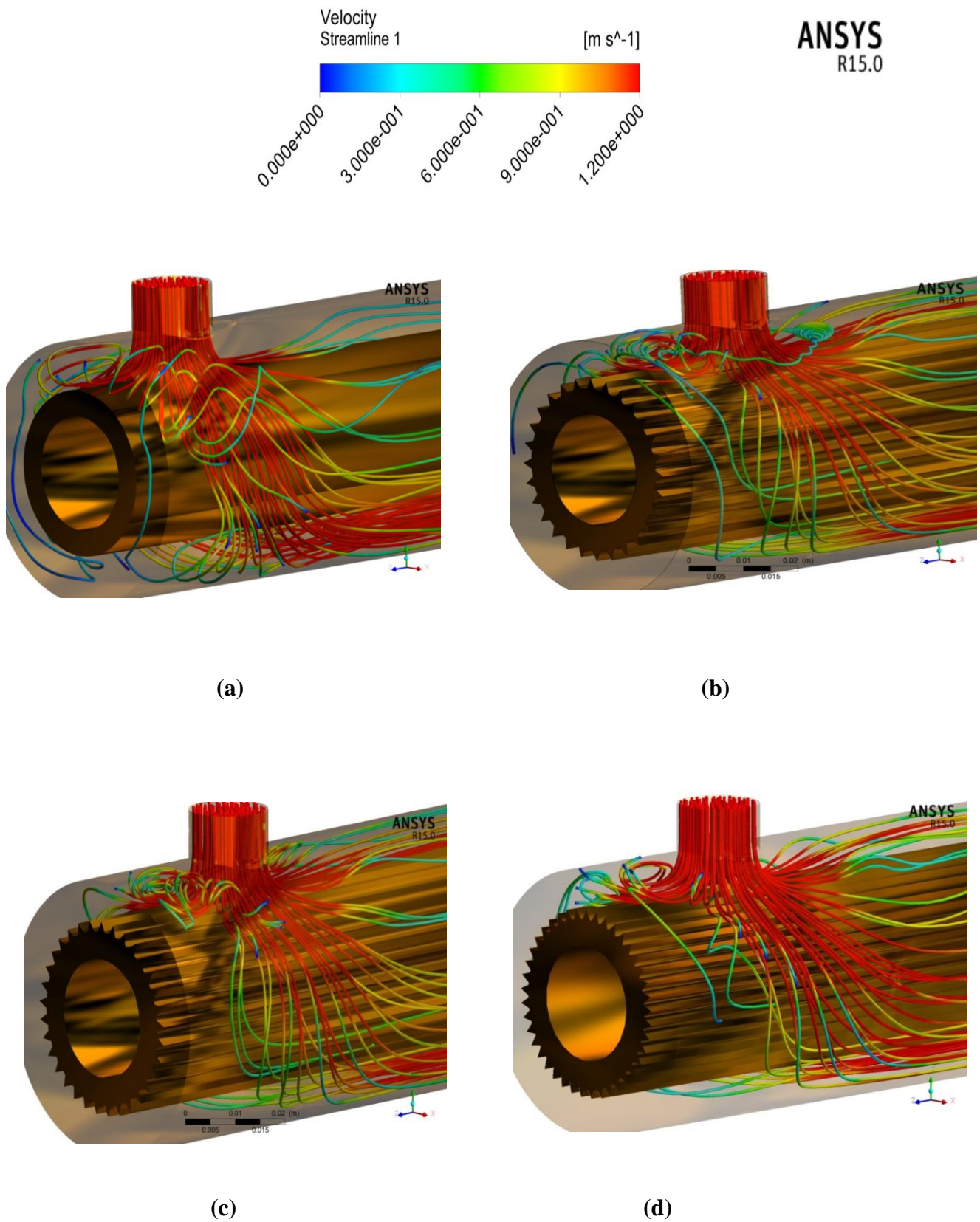


Figure (8); Streamlines for shell side entrance region with air flow over; (a) smooth tube, (b) finned tube with pitch (3.5mm), (c) finned tube with pitch (3mm), (d) finned tube with pitch (2.5mm).

The velocity contours for tube side in internal finned tube computational models (G02) and smooth tube (G04) were shown in figure (10). All these contours were taken for the same water volumetric flow rate ( $Q=10$  liter/min.) and at the axial distance (0.5m) which is located at the middle of tube at fully developed region.

As seen in the figure (10-b), the flow within longitudinal finned tube with pitch (3.5mm) which is case [G02-P3] increases velocity to 110.731% higher than that in case of smooth tube [G04] figure (10-a). This increment occurs as previously due to reduction in hydraulic diameter which leads to increase velocity at constant volumetric flow rate. In the case of G02-P2, flow within longitudinal finned tube with pitch (3mm), figure (10-c), the velocity is 124.508% higher than in flow within smooth tube and by 20.97% higher than in flow within finned tube with pitch (3.5mm). Also in the flow within longitudinal finned tube with pitch (2.5mm)[G02-P1], figure (10-d), the velocity is 136.05%, 40.52% and 19.928% higher than in cases of G04, G02-P3 and G02-P2 respectively.

explained the mean velocity propagation along the tube side at different axial locations. The velocity magnitudes satisfy continuity and momentum conservation as the solution converged in *ANSYS solver*, the differentiations between cases return to the fact that as pitch decreases between fins lead to increase fins number and as a result, a reduction in water cross sectional area with increasing velocity and decreasing of hydraulic diameter for a constant Reynolds number.

Table (3). Velocity magnitudes for different axial locations within tube side with water flow inside smooth and finned tubes.

Case	Velocity magnitude (m/s)				
	0.0m (Water Inlet)	0.25m	0.5m	0.75m	1.0m (Water Outlet)
Smooth tube (G04)	0.4384	0.4384	0.4384	0.4384	0.4384
Finned tube with pitch (3.5mm) (G02-P3)	1.5268	1.5268	1.5268	1.5268	1.5268
Finned tube with pitch (3mm) (G02-P2)	1.8845	1.8845	1.8845	1.8845	1.8845
Finned tube with pitch (2.5mm) (G02-P1)	2.3016	2.3016	2.3016	2.3016	2.3016

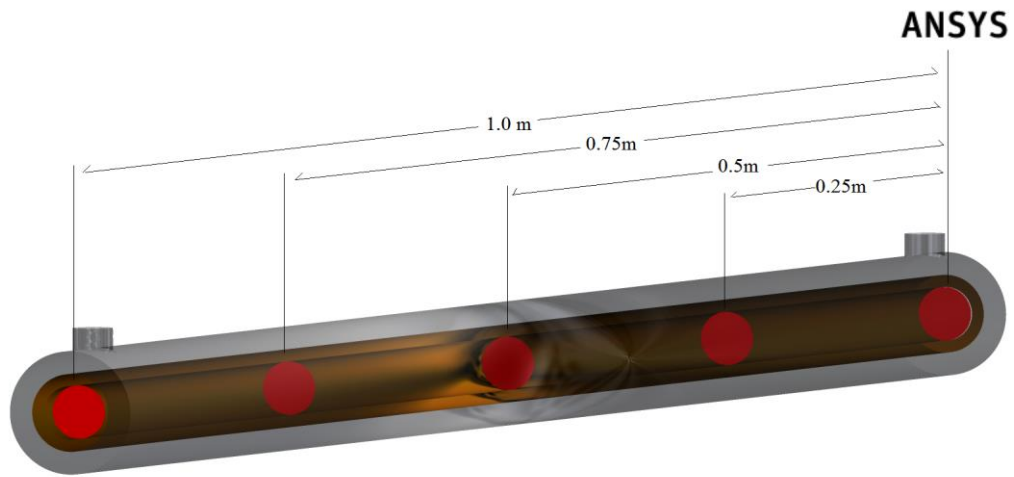
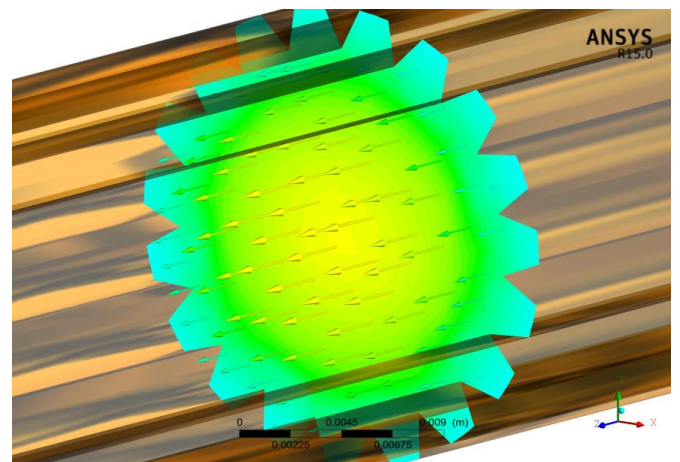
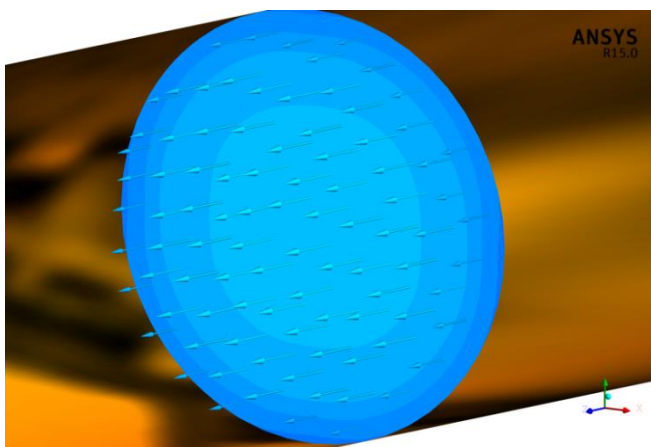
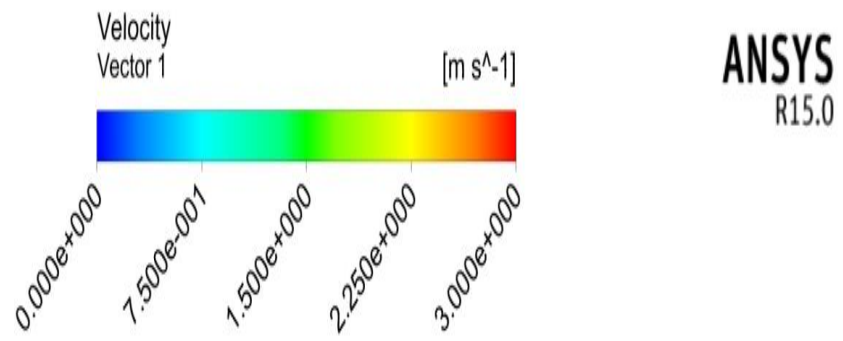
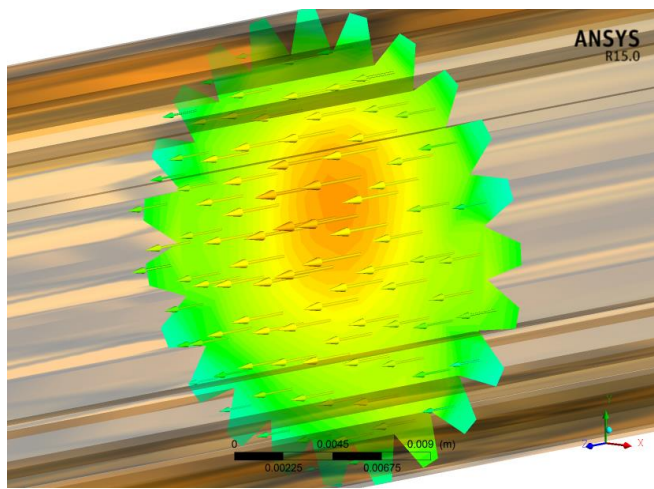
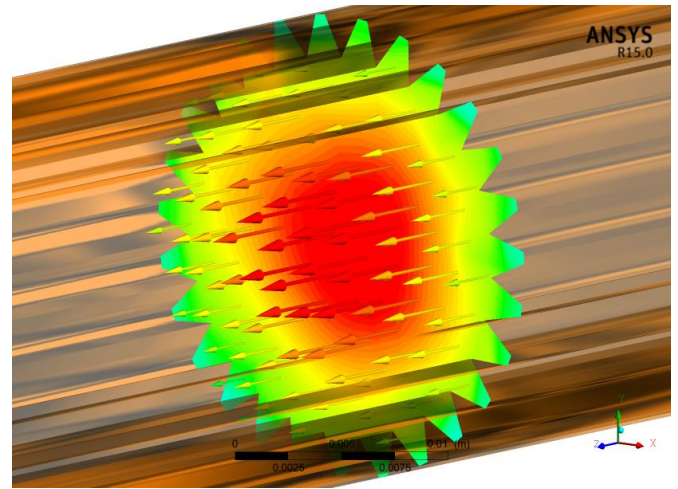


Figure (9). axial locations within tube side





(c)



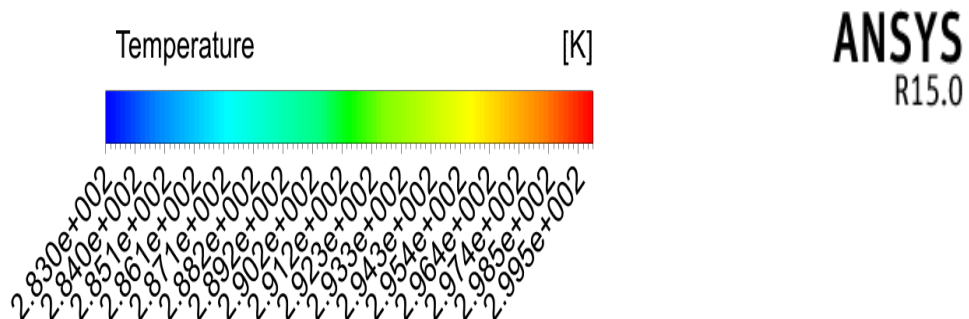
(d)

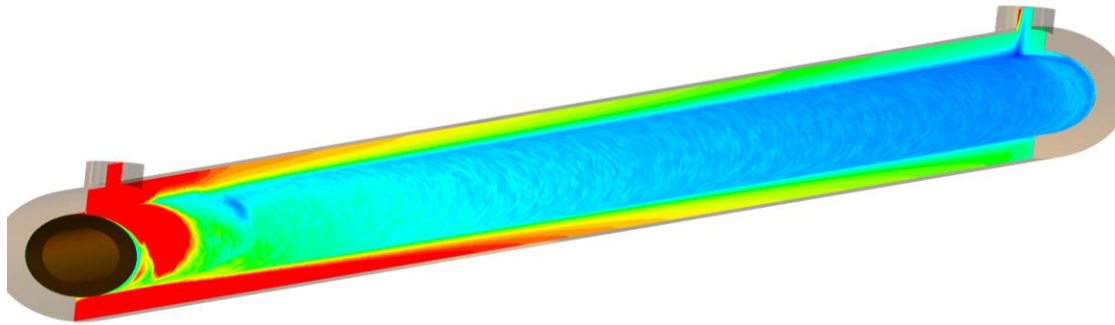
Figure (10). Velocity contours for tube side with water flow within; (a) smooth tube, (b) internal finned tube with pitch (3.5mm), (c) internal finned tube with pitch (3mm), (d) internal finned tube with pitch (2.5mm).

### 7.2 Temperature Distribution

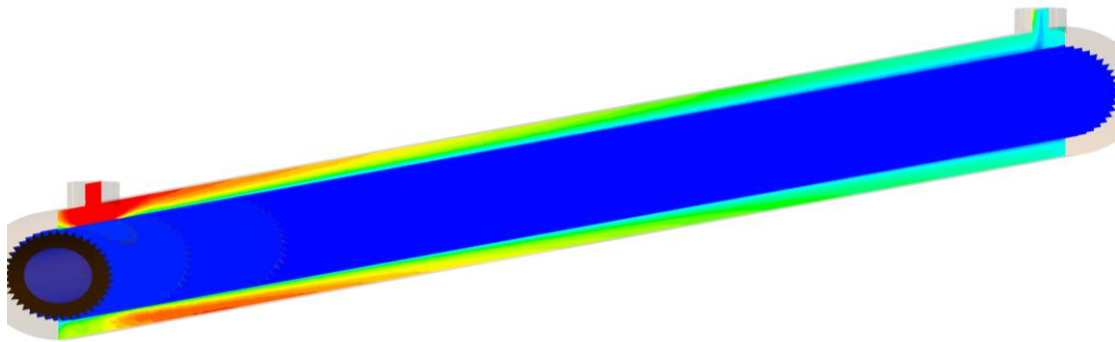
The variations in temperature difference for the computational domains are examined. The results are reported in the form of temperature contours at along whole the axial direction.

Temperature contours are shown in figures(9,10,11,12) for the shell side in all computational domains considered at same inlet air velocity (4 m/s) and along whole the axial direction.



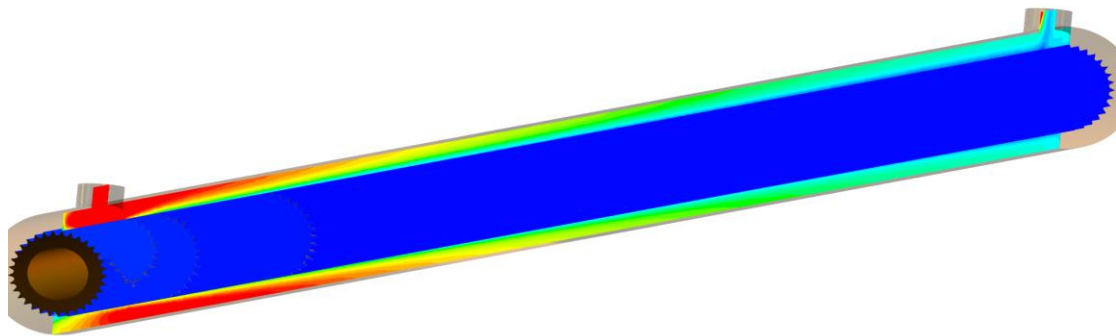


(a) Flow over smooth tube [G04].

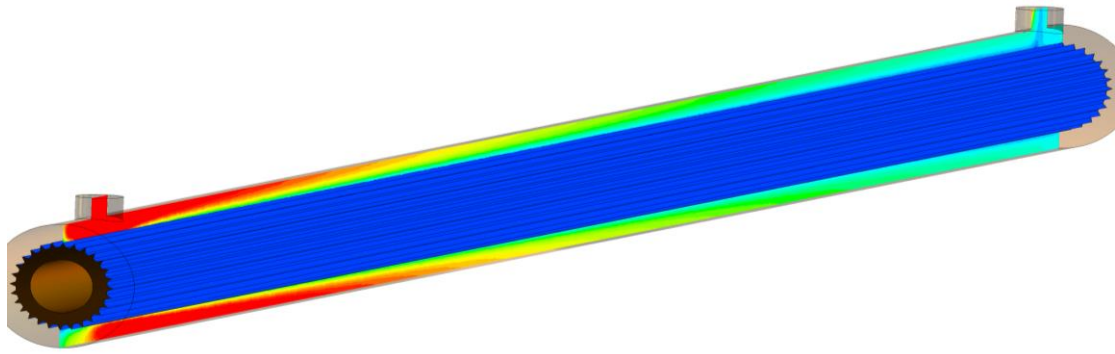


(b) Flow over external finned tube with pitch 2.5mm [G01-P1].

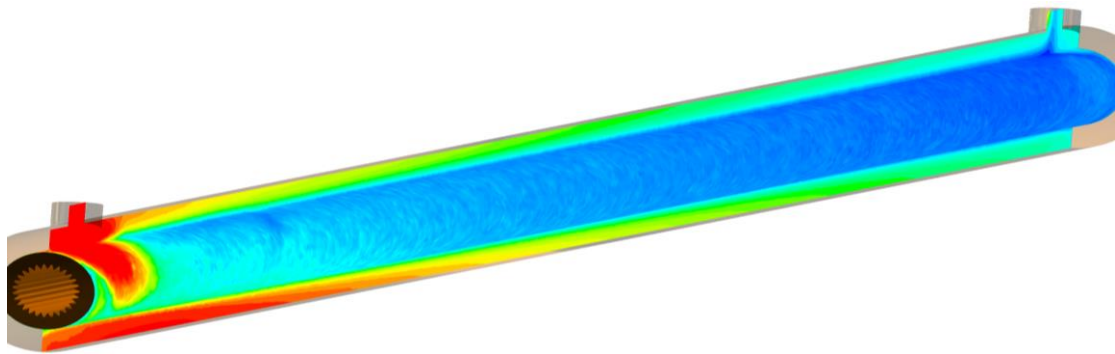
Figure (11); Temperature contours for shell side with air flow at (4 m/s inlet).



(a) Flow over external finned tube with pitch 3.0mm [G01-P2].

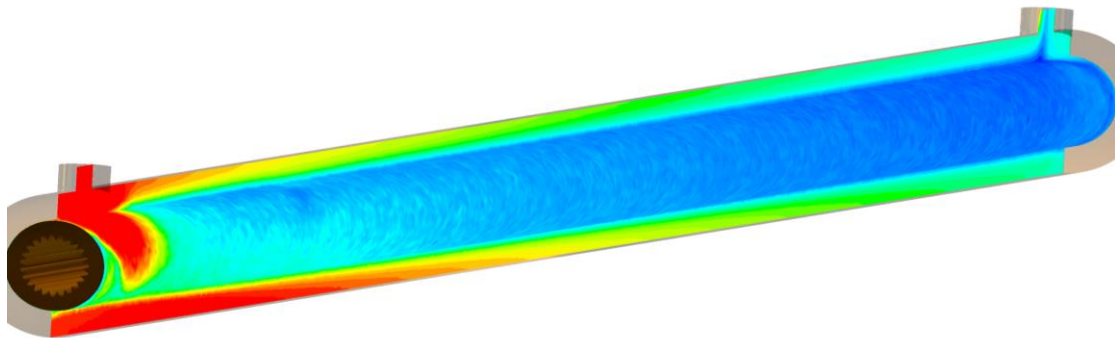


(b) Flow over external finned tube with pitch 3.5mm [G01-P3].



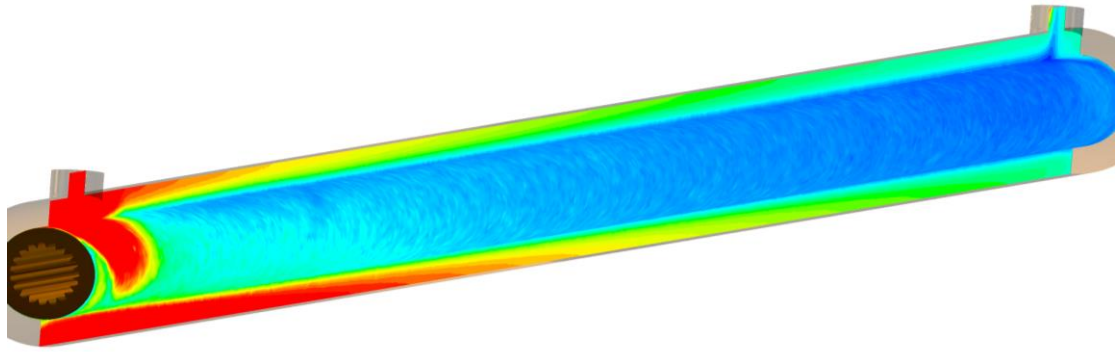
(c) Flow over internal finned tube with pitch 2.5mm [G02-P1].

Figure (12); Temperature contours for shell side with air flow at (4 m/s inlet).

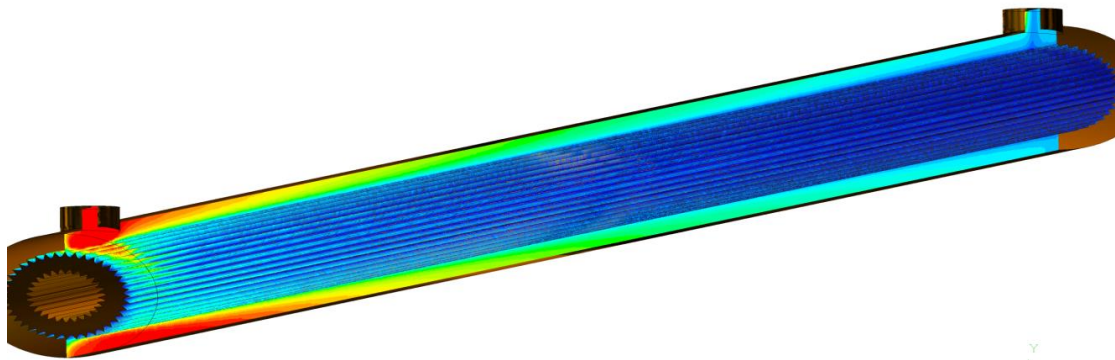


(a) Flow over internal finned tube with pitch 3.0mm [G02-P2].



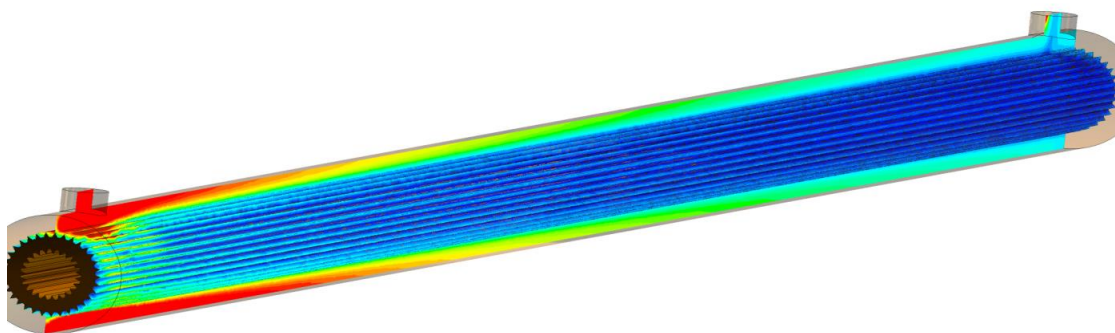


(b) Flow over internal finned tube with pitch 3.5mm [G02-P3].

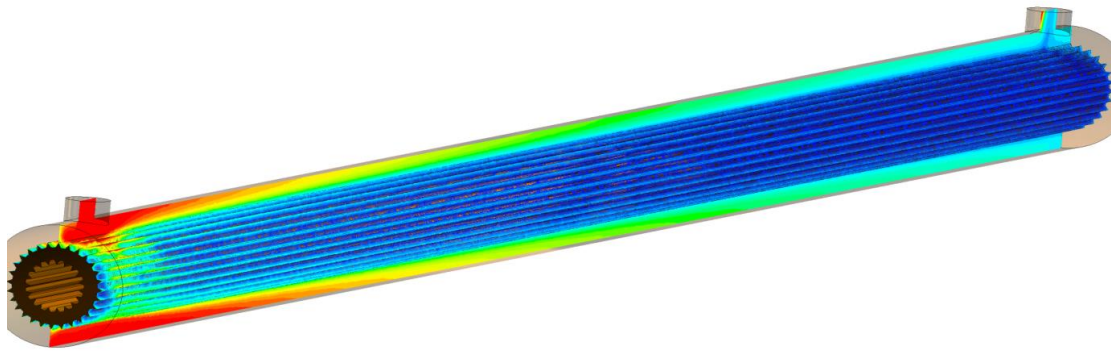


(c) Flow over finned surfaces tube with pitch 2.5mm [G03-P1].

Figure (13); Temperature contours for shell side with air flow at (4 m/s inlet).



(a) Flow over finned surfaces tube with pitch 3.0mm [G03-P2].



(b) Flow over finned surfaces tube with pitch 3.5mm [G03-P3].

Figure (14); Temperature contours for shell side with air flow at (4 m/s inlet).

## 8. Conclusions

This work presented both experimental and numerical investigation of heat transfer performance of longitudinal fins with and without high integral fin tubes. Also, using two type of fluid in inner tube is cold water and annular tube is hot air in the present heat exchanger. The main concluded points of this study may be summarized as follows:

1. Results of numerical simulation showed that adding fins would enhance heat dissipation through heat exchanger. It is noted that heat transfer behavior increases within present model as air mass flow rates and water Reynold's numbers increases. Heat transfer enhancement by adding triangular fins to mixed (outer and inner) surface tube has been found during numerical simulation. Is successful for predicting both heat transfer and fluid flow in the present heat exchanger. The heat transfer augmentation is apparent when adopting fins on (outer and inner) surface of inner tube in present heat exchanger.
2. The finned tubes provide higher Nusselt numbers than the smooth tube. In the less pitch ( $p=2.5\text{mm}$ ) compared with other pitch .
3. The numerical results were compared with results obtained from Dittus-Boelter. Good agreements were obtained with a maximum deviation of (10)%.
4. The results obtained from the tubes with triangular finned are compared with the smooth tube heat exchanger. It is found that the triangular finned have a significant effect on the heat transfer augmentations (47.5%, 60.5% and 67.5 %).

## 9. References

1. Bergles, A. E, (2000) "*Heat Transfer Enhancement*", in "*The CRC Handbook of Thermal Engineering*", F. Kreith (editor), CRC Press, .
2. Zimparov, V. D, Penchev, P. J. and Meyer, J., (2006) "*Performance Evaluation of Tube-in-Tube Heat Exchangers with Heat Transfer Enhancement in the Annulus*", Thermal Science, Vol. 10, pp. 45-56,

3. Jong Min Choi, Yonghan Kim, Mooyeon Lee and Yongchan Kim, (2010) "*Air Side Heat Transfer Coefficients of Discrete Plate Finned–Tube Heat Exchangers with Large Fin Pitch*", Applied Thermal Engineering, Vol.30, pp.174–180, .
4. Ayad Mezher Rahmah, (2011) "*Experimental Study of an Integral Finned–Tube Heat Exchanger*", University of Technology – Mechanical Engineering Department M.Sc., thesis, .
5. Ali S. Al-Jaberi, Majid H. M. and Bassam A. Saheb, (2014) "*circular fins with slanted blades: uniform heat flux and isothermal processes*", international journal of mechanical engineering and technology (IJMET), Volume 5, Issue 5, (pp. 133-143),
6. Bashar M. Essa, (2016) "*Experimental and Numerical Investigation To Evaluate The Performance of Triangular finned Tube Heat exchanger*" – University of Nahrain Mechanical engineering Department M.sc thesis in, .
7. Ajay K. Agrawal and Subrata Sengupta ,(1990) "*Laminar flow and heat transfer in a finned tube annulus*" , Int. J. Heat and Fluid Flow, Vol. 11, No. 1, pp. 54-59, .
8. Torikoshi, K., and Xi, G. N., (1995) "*A Numerical Study of Flow and Thermal Fields in Finned Tube Heat Exchangers (Effect of the Tube Diameter*" IMECE Proceedings of the ASME Heat Transfer Division, HTD-Vol. 317-1, pp. 453-457, .
9. Syed K. S., Mazhar Iqbal, Mir N. A., (2007) "*Convective Heat Transfer in the Thermal Region of Finned Double–pipe*", Heat Mass Transfer, Vol.43, pp.449–457,.
10. Iqbal Z., Syed K. S., Ishaq M., (2013) "*Optimal Fin Shape in Finned Double Pipe with Fully Developed Laminar Flow*", Applied Thermal Engineering, Vol.51, pp.1202-1223,
11. Lars Davidson, (2009) "*An Introduction to Turbulence Models*", Department of Thermo and fluid dynamics, Chalmers University of Technology, Sweden, .
12. B. Yu, J. H. Nie, Q. W. Wang, W. Q. Tao, (1999) "*Experimental study on the pressure drop and heat transfer characteristics of tubes with internal wave-like longitudinal fins*", Heat and Mass Transfer 35 (1999) 65 ± 73 Ó Springer-Verlag, .